Paper

COMPARISON OF TWO LEG PHANTOMS CONTAINING ^{241}AM IN BONE

Gary H. Kramer,* Barry Hauck,* Kevin Capello,* Werner Rühm,† Nabil El-Faramawy,†‡ David Broggio,§ Didier Franck,§ Maria Antonia Lopez,** Teresa Navarro,** Juan Francisco Navarro,** Begoña Perez,** and Sergei Tolmachev††

Abstract—**Three facilities (CIEMAT, HMGU and HML) have used their in vivo counters to compare two leg phantoms. One was commercially produced with ^{241}Am activity artificially added to the bone inserts. The other, the United States Transuranium and Uranium Registries' (USTUR) leg phantom, was manufactured from ^{241}Am-contaminated bones resulting from an intake. The comparison of the two types of leg phantoms showed that the two phantoms are not similar in their activity distributions. An error in a bone activity estimate could be quite large if the commercial leg phantom is used to estimate what is contained in the USTUR leg phantom and, consequently, a real person. As the latter phantom was created as a result of a real contamination, it is deemed to be the more representative of what would actually happen if a person were internally contaminated with ^{241}Am.**

Health Phys. 101(3):248–258; 2011

Key words: ^{241}Am; bones, human; calibration; dosimetry, internal

INTRODUCTION

The Human Monitoring Laboratory (HML), which operates the Canadian National Calibration Reference Centre for Bioassay and In vivo Monitoring (Kramer and Limson Zamora 1994; Daka and Kramer 2009), has collaborated with Helmholtz Zentrum München–Deutsches Forschungszentrum für Gesundheit und Umwelt (HMGU) in Germany and the Centro de Investigaciones Energéticas, Medioambientales y Tecnológicas (CIEMAT) in Spain to compare the counting characteristics of the United States Uranium and Transuranium Registries' (USTUR) leg phantom held at the United States Department of Energy's Phantom Library (U.S. DOE 2009) with those of other commercially-available phantoms. The USTUR phantom, the subject of a complete *Health Physics* journal issue (Breitenstein et al. 1985), has had the ^{241}Am deposited in bone through a normal metabolic process resulting in an activity distribution that is representative of what may be expected in an exposed human male.

Each facility has also previously made measurements on a commercially-available leg phantom (not necessarily the same phantom for each facility but all from the same supplier). The commercially-available phantom had the ^{241}Am artificially distributed in the bone substitute material unlike the USTUR phantom. All three facilities use their partial body or lung counters for the measurement of radioactivity in bone. While each is based on hyperpure germanium, the details of each facility are somewhat different. This paper presents the results of the comparison of the two types of leg phantoms and shows that the two phantom types (commercial vs. USTUR) are not similar in their activity distributions.

MATERIALS AND METHODS

Human monitoring laboratory

Lung counter. The detectors used were developed by ORTEC (Ortec 2010a) using a new front contact technology. This new technology provides excellent energy resolution and peak shape at low energies with large area detectors, which makes them very interesting

* Human Monitoring Laboratory, Radiation Protection Bureau, 775 Brookfield Road, Ottawa, Ontario, K1A 1C1 Canada; † Helmholtz Zentrum München—German Research Center for Environmental Health, GmbH, Institute of Radiation Protection, Ingolstädter Landstraße 1, D-85764 Neuherberg, Germany; ‡ On leave from Department of Physics, Faculty of Science, Ain Shams University, 65511 Abbassia, Cairo, Egypt; § Institut de Radioprotection et de Sûreté Nucléaire, Internal Dose Assessment Laboratory, DRPH/SDI/LEDI, BP-17 F-92262 Fontenay-aux-Roses Cedex, France; ** Centro de Investigaciones Energéticas, Medioambientales y Tecnológicas, Avda. Complutense, 22, Madrid 28040, Spain; †† United States Transuranium and Uranium Registries, Washington State University, 2340 Lindberg Loop, Richland, WA 99354.

For correspondence or reprints contact: Gary H. Kramer, Human Monitoring Laboratory, Radiation Protection Bureau, 775 Brookfield Road, Ottawa, Ontario, K1A 1C1 Canada, or email at gary.h.kramer@hc-sc.gc.ca.

(*Manuscript accepted* 20 *January* 2011)
0017-9078/11/0

DOI: 10.1097/HP.0b013e3182118f61

for lung burden studies. These detectors also exhibit excellent energy resolution and peak shape at high energies (1 MeV). Each of the four detectors contains a germanium crystal that is 85 mm in diameter and 30 mm in thickness. The entrance window is 0.76 mm carbon fiber and is 5 mm from the germanium crystal. Each detector is cooled with a large dewar that holds 17.5 L of liquid nitrogen with a holding time of 8 d. The detectors are housed in a low background steel chamber (described below) suspended from a track that allows the detectors to be moved independently in five of the six motions that are possible. Vertical and horizontal movements are manual, either by a hand-wheel (vertical) or by simply pushing the detector track mount (horizontal) along the main track (front to back) or across the joining track (side to side). The two horizontal rotational movements are electrically driven using actuators. Rotation about the vertical axis is manual.

The lung counter's electronics were configured to collect 16,384 channels of data for each detector. The energy calibration is ~0.03 keV per channel, giving a maximum energy of 480 keV. The efficiency calibration and analysis of spectral data were performed using Ortec's Renaissance 32 software.

Counting chamber. The inside dimensions of the chamber are 1.52 m × 2.13 m × 2.13 m, and access is through a set of double doors that are operated by electric motors controlled from the laboratory. There is also a large water-filled window of dimensions 0.3 m × 0.46 m × 0.6 m wide and two small access ports through the walls for cabling, ventilation, etc. The thickness of the chamber walls, floor and ceiling is 0.2 m, and the approximate weight of the chamber is 51 metric tons. The inner surfaces of the room are covered by 6.3 mm of lead that reduces the background (below 0.1 MeV) by a factor of two. An additional graded Z liner consisting of tin (0.08 cm thick) and copper (0.18 cm thick) was added at the same time as the counting system was installed.

Helmholtz Zentrum München

Partial body counter. The HMGU partial body counter includes four different high-purity Germanium detectors. These detectors are independently mounted on pillars to allow manual adjustment to any 3D geometry required for a measurement.

Detectors #2 and #3 each consist of a crystal with a diameter of 50 mm and a thickness of 10 mm, while detector #6 uses a crystal with a diameter of 71 mm and a thickness of 30 mm. Detector #4 (Canberra Semiconductor NV/SA, Z.1. Researchpark 80, 1731 Zellik, Belgium), which was used for the present work, includes a crystal with a diameter of 81 mm and a thickness of 22 mm (Canberra 2010). The crystal is located 5 mm from the entrance window, which is made of carbon epoxy (thickness of 0.5 mm). This detector is particularly suitable to detect photons with low energies with a high detection efficiency. The energy resolutions (full width half maximum) of this detector as guaranteed by the manufacturer are 500 eV at 5.9 keV, 660 eV at 59.5 keV, 750 eV at 122 keV and 2.2 keV at 1332.5 keV, respectively. The detector is operated at a voltage of +4,000 V.

The signals from detector #4 were amplified by a Canberra AFT Research Amplifier (model 2025) and then processed by using a EG&G ORTEC Spectrum Master 919. All spectra were analyzed using the ORTEC GammaVision software from Advanced Measurement Technology.

Counting chamber. The detectors are located inside a massive shielding chamber (Fig. 1). The entrance is formed as a labyrinth, and the dimensions of the inner chamber are 3 m × 1.5 m × 2.1 m. From inside to outside, it is shielded by 2 mm of copper, 4 mm of lead and 140 mm of steel. The shielding chamber is about 8 m below the surface of the earth to provide additional shielding against cosmic radiation. The facility is described in more detail elsewhere (Wahl et al. 2002).

CIEMAT (Centro de Investigaciones Energéticas, Medioambientales y Tecnologicas)

Lung counter. The CIEMAT lung detector system was used to perform the measurement of ^{241}Am in the leg phantom. This detector system consists of four Low Energy (LE) Ge (Canberra 2010) detectors mounted in a two-ACTII array configuration. The active area of each

Fig. 1. HMGU's counting chamber that can be used for in vivo counting. In this picture, one detector is being used to measure the ^{241}Am in the phantom's bone.

detector is 3,800 mm^2, with a diameter of 70 mm, thickness of 25 mm and a carbon fiber window 0.5 mm thick. The LEGe system is defined as four inputs or individual detectors, each being set for a 4,096 channel acquisition region and amplifier gain of 0.267 keV/channel in an analysis energy range of 10–1,000 keV. The configuration of the counting system incorporates three Detector Groups: the All Summed group is defined as the sum of the four germanium detectors' spectra, Det1-2 is the sum of the two individual detectors over the right lung, and the Det 3-4 group corresponds with the left lung. Thus, the final result of a lung measurement is analyzed for each spectrum from individual detectors and for the three composed spectra, obtaining information about the distribution of the contaminant in the lung area. The detector arrangements used in this work are described below.

Counting chamber. The detectors are installed inside a chamber of 2.43 m × 2.43 m × 1.97 m, built with the following materials: 13-cm pre-World War II steel walls lined with 5 mm Pb, 1 mm Cd and 1 mm Cu. The room is in "over-pressure" and has a ventilation system with "absolute" filters, supplying 30 cycles/hour and constant humidity and temperature (21°C).

The phantoms

The commercial leg phantom. The International Atomic Energy Agency supplied the HML with a phantom representing a human knee that had been built in the United States (Spitz et al. 2000) (see Fig. 2). The leg phantom consists of a solid, polyurethane-based shell, in which part of a tibia, fibula and femur made from a cortical bone substitute material and containing a known quantity radionuclide, can easily be inserted. There is no patella. The phantom came with four bone sets containing no activity, ^{241}Am 30.3 kBq (23 May 2000), ^{152}Eu and ^{210}Pb. Only the ^{241}Am results are considered in this paper.

CIEMAT acquired its own commercial leg calibration phantom from the University of Cincinnati (U.S.A.). This phantom's ^{241}Am content was 33.8 kBq. This phantom was sent from CIEMAT to HMGU, Germany, in October 2007 and measured at both facilities. Thus, HML measured a different leg phantom from the same commercial supplier to CIEMAT and HMGU, although they are built to the same specifications and should, in theory, be identical in their performance characteristics.

USTUR leg phantom. This phantom is part of a larger phantom that represents a whole body. It came to the USDOE Phantom Library from the USTUR. The donor, Stuart E. Gunn, was a research chemist who had a significant, long-standing internal deposition of ^{241}Am (USTUR 0102 Narrative 2009). The entire October 1985 issue of *Health Physics* (Bretenstein et al. 1985) was devoted to data from this case. Half of Gunn's skeleton was encased in tissue-equivalent plastic. This unique anthropomorphic phantom can be used for calibrating whole body counting systems at USDOE laboratories and others.

The USTUR bone phantom consists of four sections: a head (skull) phantom, a chest/torso phantom, a left arm phantom and a left leg phantom (Fig. 3). With the exception of the skull, each labeled skeleton half is the left side. Use of each phantom section may require "double" counts, one for each side of the bilateral symmetry, in order to compensate for the unlabeled skeleton halves. The half of the skeleton that was radiochemically analyzed gave a total content for the

Fig. 2. The commercial knee phantom borrowed from the IAEA showing the insert sets.

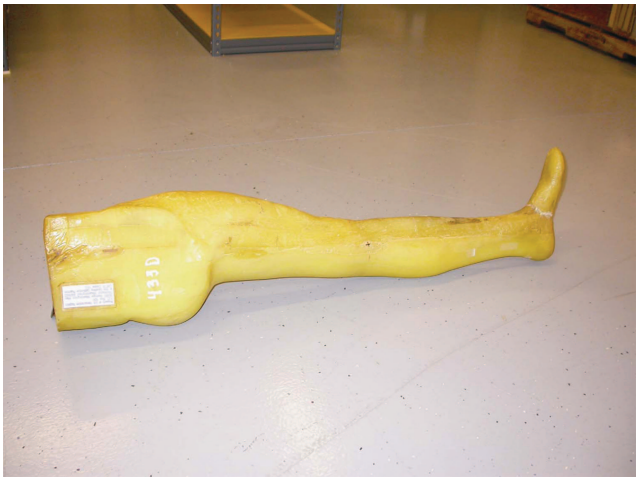

Fig. 3. The USTUR bone phantom.

Table 1. Revised activities of the USTUR/DOE Leg Phantom—Ref Date 1 February 1980; details are given elsewhere (USTUR 2010).

Bone sample	Weight (g)	^{241}Am, Bq kg^{-1} wet		^{241}Am activity, Bq	
		Value	sd[a]	Value	sd
Phantom[a]	1965.6			1243.4	10.9
Leg (L)	1325.6			856.5	9.5
Femur (L)	685.7			504.5	*8.4*
PE	*199.8*	*577.7*	*20.7*	*115.4*	*4.1*
PS	*123.1*	*791.5*	*24.7*	*97.4*	*3.0*
MS	*104.2*	*815.6*	*32.0*	*85.0*	*3.3*
DS	*129.8*	*656.8*	*26.5*	*85.3*	*3.4*
DE	*128.8*	*942.5*	*35.9*	*121.4*	*4.6*
Tibia (L)	*500.8*			*271.5*	*4.2*
PE	*153.4*	*554.7*	*13.7*	*85.1*	*2.1*
PS	*162.6*	*534.1*	*17.4*	*86.9*	*2.8*
DS	*116.2*	*505.7*	*12.9*	*58.8*	*1.5*
DE	*68.6*	*594.9*	*23.4*	*40.8*	*1.6*
Fibula (L)	*103.9*			*60.4*	*1.4*
PE	*17.8*	*758.3*	*44.2*	*13.5*	*0.8*
PS	*42.0*	*443.7*	*19.5*	*18.6*	*0.8*
DS	*31.3*	*638.1*	*26.4*	*20.0*	*0.8*
DE	*12.9*	*647.1*	*23.9*	*8.3*	*0.3*
Patella (L)	*35.2*	*571.7*	*23.6*	*20.1*	*0.8*
Pelvis (L)[a]	*374.0*			*173.3*	*4.3*
Ilium	*175.2*	*521.5*	*20.4*	*91.4*	*3.6*
Ischium	*162.4*	*503.8*	*14.2*	*81.8*	*2.3*
Fluids	*36.4*	*2.47*	*0.22*	*0.090*	*0.008*
Foot & Ankle (L)	*266.0*			*213.7*	*3.3*
Tarsals	*179.9*			*141.1*	*3.1*
Talus	57.2	708.9	27.7	40.6	1.6
Calcancus	65.3	877.2	38.3	57.3	2.5
Cuboid	18.2	739.4	31.9	13.4	0.6
Navicular	15.0	739.6	33.5	11.1	0.5
Cuneiform Medial	10.8	577.6	22.1	6.3	0.2
Cuneiform Intermediate	5.5	1014.3	42.0	5.6	0.2
Cuneiform Lateral	7.8	872.5	33.0	6.8	0.3
Metatarsus	*60.6*			*53.0*	*1.0*
Metatarsal-1	19.0	857.8	34.0	16.3	0.6
Metatarsal-2	11.2	943.2	40.0	10.5	0.4
Metatarsal-3	12.8	858.7	36.4	11.0	0.5
Metatarsal-4	8.9	770.0	32.2	6.9	0.3
Metatarsal-5	8.7	958.3	40.5	8.4	0.4
Phalanges	*25.5*			*19.5*	*0.3*
Proximal-1	6.7	914.5	32.8	6.12	0.22
Proximal-2	2.4	1000.2	45.1	2.41	0.11
Proximal-3	1.8	937.7	47.8	1.70	0.09
Proximal-4	1.8	913.7	31.3	1.65	0.06
Proximal-5	1.2	1044.1	46.9	1.29	0.06
Proximal, total	*14.0*			*13.2*	*0.3*
Middle-2	0.8	965.8	45.9	0.79	0.04
Middle-3	0.6	852.0	58.2	0.53	0.04
Middle-4	0.5	868.5	56.9	0.43	0.03
Middle-5	0.1	1512.8	100.0	0.21	0.01
Middle, total	*2.1*			*1.96*	*0.06*
Distal-1	7.3	353.6	11.6	2.58	0.08
Distal-2	0.6	762.9	31.0	0.49	0.02
Distal-3	0.7	761.5	32.3	0.52	0.02
Distal-4	0.5	815.2	36.9	0.38	0.02
Distal-5	0.4	1172.2	52.0	0.41	0.02
Distal, total	*9.5*			*4.39*	*0.09*

[a] 67% confidence interval of the sample count is due to uncertainties in counter backgrounds and counter efficiencies for measuring the sample and in the calibration of the ^{243}Am tracer.

entire skeleton, assuming bilateral symmetry of activity of 4,407 Bq (4,219 Bq on 1 Jan 2007). Detailed analysis of the activity distribution of the radiochemically analyzed bone is found elsewhere (Breitenstein et al. 1985; Hickman and Cohen 1988; Lynch 1988). Since that time, errors have been found in the activity assignment of the bones of the phantom. A recent re-evaluation of the phantom's activity is given in Table 1 (USTUR 0102 Radiochemistry 2010), and a discussion of this re-evaluation will be published elsewhere. The ^{241}Am activity in the leg was 1,243.5 Bq on 1 Feb 1980 (i.e., 1,190.6 Bq in 2007 at the time of the measurement).

Counting protocol. The commercial knee phantom was measured with the ^{241}Am bone set with the detector placed in different positions over the leg. The small lengths of the bone inserts in the commercial phantom limit the number of counting positions available, unlike the USTUR phantom that contains all the bones of a human leg. Note that the USTUR leg phantom has no interchangeable bone sets.

Human monitoring laboratory. The reference point for the counts on the IAEA's commercial leg phantom was the center of the detector's entrance window relative the center of the knee cap (see Fig. 4). Four counting geometries were defined: 4 cm above the knee, centered on the kneecap (the reference point), 4 cm below the knee and 8 cm below the knee. Each count was 60,000 s.

The USTUR leg phantom was measured with one detector placed in different positions over the leg. The first counting position was 26 cm from the middle of the foot to the edge of the detector. The detector was tangential to the surface of the top of the leg. Thirteen other counts were performed with the detector being moved incrementally higher every 4 cm on the leg, except near the knee when the increment was shortened to 1 cm until it was 62 cm from the foot. Each count was 60,000 s except for the measurement at position 6. That was 300,000 s to take advantage of a weekend count.

Helmholtz Zentrum München. For all measurements, the distance of the detector surface to the knee surface was chosen to be about 1 cm. In all cases, detector #4 was surrounded by a lead collimator with a thickness of 1 mm to minimize contribution from scattered photons. This was done to increase the spatial resolution of the detector, which was of some importance for the scans performed along the leg phantom. The length of the shield was 13 cm covering 12 cm of the detector. The front of the lead shield consisted of a ring with a thickness of 1 cm (Fig. 5).

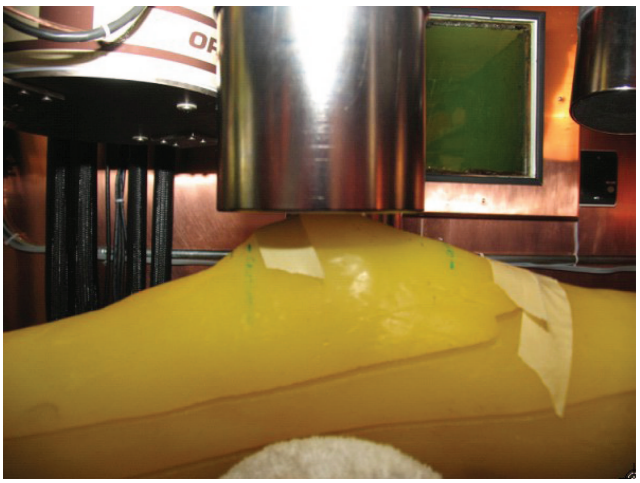

Fig. 4. Commercial knee phantom measured at the reference point in the HML.

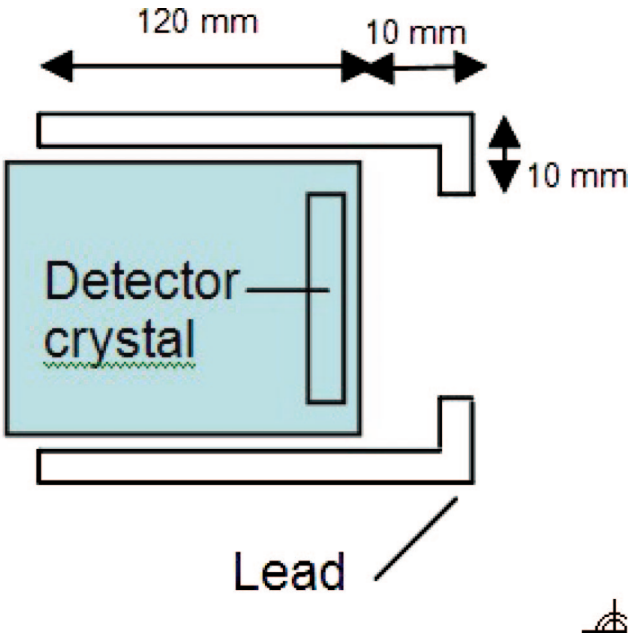

Fig. 5. Sketch of the HMGU detector geometry including the lead shield (not drawn to scale).

For the commercial leg phantom, two independent vertical scans were performed with detector #4. As usual, the protective plastic cap that is usually used during person measurements was removed, but the lead collimator remained in place. A distance of 1 cm was kept between the surface of the phantom and the detector. Measurements were made along the central axis from 16 cm above the kneecap to 25 cm below the kneecap. With a chosen counting time of 1,000 s, the net counts in the 60 keV peak varied from about 20,000 to 150,000, so the counting statistics are better than 1%.

The same configuration (detector #4, no plastic cap but lead collimator, distance to the knee, vertical scan)

was also used for the USTUR leg phantom. In this case, a counting time of 5,000 s was chosen, which resulted in net counts in the 60 keV peak between 330 (at position 73.8 cm) and 9,700 (at position 49.8 cm), depending on the detector position above the leg phantom.

CIEMAT (Centro de Investigaciones Energéticas, Medioambientales y Tecnologicas)

To provide the most realistic counting geometry for in vivo knee calibration, the LLNL (Lawrence Livermore National Laboratory) torso phantom containing a "blank lungs" set was placed on the reclined dentist-chair together with two knee phantoms (CIEMAT and IAEA), each containing ^{241}Am in the bone-equivalent material. Each cryostat cooling a pair of LEGe detectors was placed above each commercial leg phantom, with a detector-knee distance of 2 cm. A calibration factor was obtained using the four LEGe detectors for measuring the two knees simultaneously for the in vivo measurement of ^{241}Am (59.5 keV); see Lopez et al. (2004).

A counting efficiency study was carried out using Monte Carlo calculations for efficiency optimization to find the "best counting geometry" (Moraleda et al. 2005) for in vivo measurement of ^{241}Am in the knee. The conclusion of this Monte Carlo study was that the maximum 59.5 keV photon fluence value is in the lower segment of the knee at an angle of 45° toward its inner side. Based on this calculational study, a counting geometry for in vivo determination of ^{241}Am in bone was selected for routine monitoring at CIEMAT WBC (Navarro et al. 2007; Lopez et al. 2010). This "wrapping counting geometry" consisted of four LEGe detectors centered along the long axis of the commercial leg phantom, placed over the lower part of the knee parallel to the tibia and fibula, wrapping the maximum area of photon emissions and setting a distance of 4 cm as the reference detector-source distance (Fig. 6).

The USTUR leg phantom was measured at CIEMAT WBC laboratory with one LEGe detector placed in different positions over the leg in a vertical position at 2 cm above the leg phantom to study the efficiency pattern. References were taken from upper-leg to foot along the USTUR leg phantom.

RESULTS AND DISCUSSION

Counting efficiency

All phantoms represent a human leg; however, the commercial phantoms only contain bones around the knee joint, and the shape of the phantom is of a bent knee. In contrast, the USTUR leg phantom consists of the bones of a whole human leg, and it is extended straight. A detector placed over the knee of the commercial phantom will receive fewer counts from the adjacent bones due to the bend in the knee, whereas the contrary is true for the USTUR leg phantom. The commercial phantom also has no patella, but this is a small defect (some ^{241}Am was found in the human bone patella of the USTUR leg phantom; see Table 1).

An analysis of the efficiency pattern of the USTUR phantom, as discussed below, showed a maximum efficiency value for center-knee position. This conclusion

Fig. 6. In vivo monitoring of USTUR leg phantom at CIEMAT: (1) vertical position of two-detector array and (2) wrapping counting geometry of four LEGe detectors.

Table 2. Results of measuring the ^{241}Am bone set in the commercial leg phantom at 59.5 keV at counting positions relative to the center of the knee cap, using one Ge vertical detector. Negative position indicates placement above the knee cap (toward the hips). Statistical uncertainties of the measurements are less than 1% for HML, HMGU, and CIEMAT.

	Efficiency (cps/photon)			
Position (cm)	HML	HMGU #1	HMGU #2	CIEMAT
−16			1.68×10^{-3}	
−15		1.82×10^{-3}		
−10		3.65×10^{-3}		
−8			4.62×10^{-3}	
−5		5.08×10^{-3}		
−4	5.79×10^{-3}			3.53×10^{-3}
0	8.42×10^{-3}	6.46×10^{-3}	7.85×10^{-3}	
4	1.41×10^{-2}			6.93×10^{-3}
5		1.07×10^{-2}		
8	1.54×10^{-2}		1.22×10^{-2}	
10		1.23×10^{-2}		
15		1.03×10^{-2}		
16			9.54×10^{-3}	
20		8.55×10^{-3}		
24			5.76×10^{-3}	
25		4.84×10^{-3}		

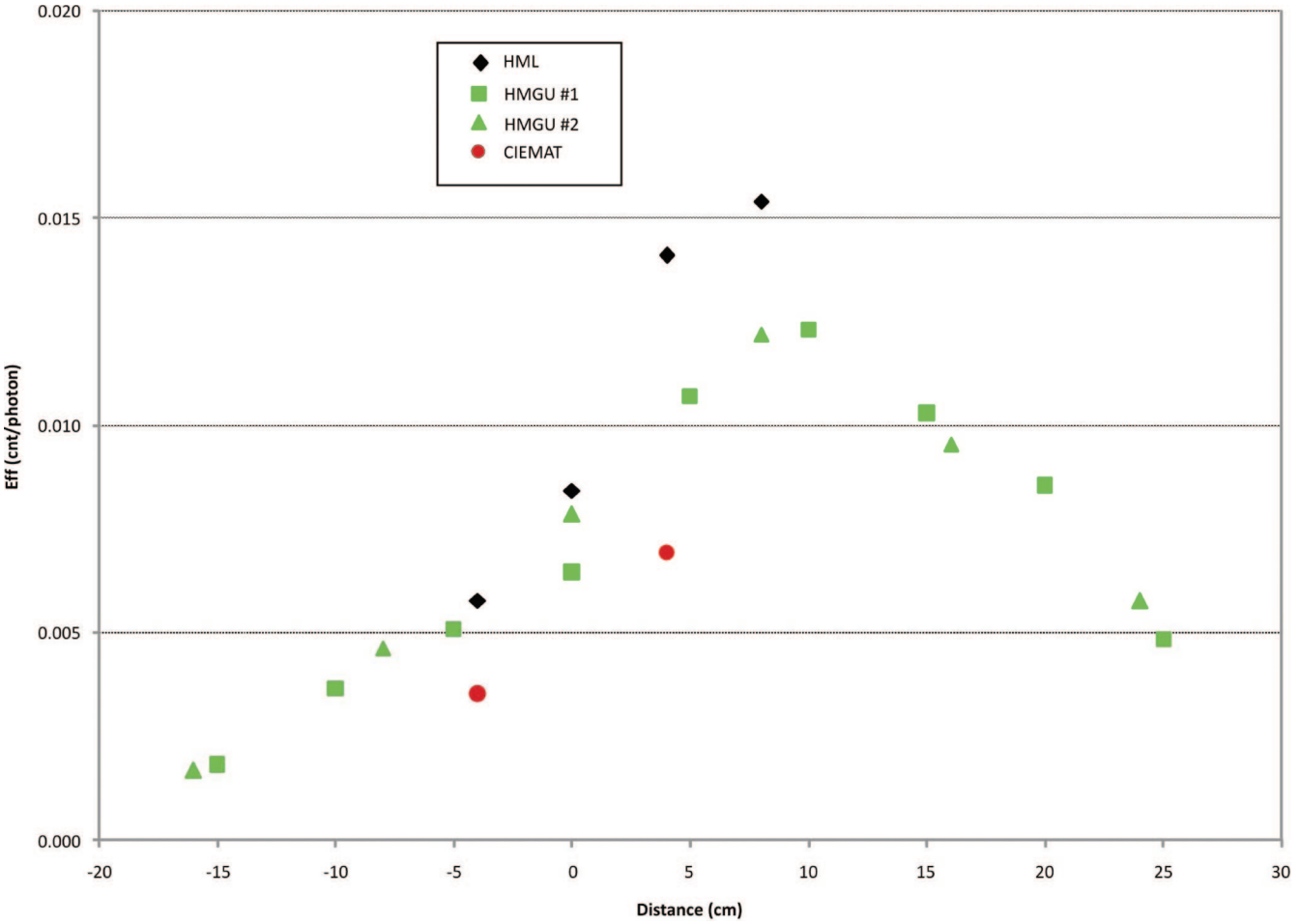

Fig. 7. Counting efficiencies of the commercial leg phantom as a function of distance from the knee cap.

Table 3. Results of measuring the ^{241}Am in the USTUR leg phantom at 59.5 keV at counting positions relative to the center of the bottom of the foot and to the detector center. Uncertainties are 2–4% and correspond to 1σ counting statistics.

HML		HMGU		CIEMAT	
Position (cm)	CE (cnt/photon)	Position (cm)	CE (cnt/photon)	Position (cm)	CE (cnt/photon)
31.3	2.44×10^{-3}	25.8	1.56×10^{-3}	25.8	1.62×10^{-3}
35.3	2.51×10^{-3}	33.8	1.34×10^{-3}	33.8	2.10×10^{-3}
39.3	2.90×10^{-3}	41.8	2.68×10^{-3}	45.8	3.09×10^{-3}
43.3	4.09×10^{-3}	49.8	4.52×10^{-3}	53.8	1.61×10^{-3}
47.3	5.65×10^{-3}	57.8	1.05×10^{-3}	60	7.15×10^{-4}
48.3	5.76×10^{-3}	65.8	3.35×10^{-4}	68	2.74×10^{-4}
49.3	5.81×10^{-3}	73.8	1.44×10^{-4}	80	1.53×10^{-4}
50.3	5.40×10^{-3}			88	1.40×10^{-4}
51.3	5.24×10^{-3}			100	3.77×10^{-4}
55.3	3.23×10^{-3}			108	1.52×10^{-4}
59.3	1.52×10^{-3}				
60.3	1.05×10^{-3}				
63.3	6.71×10^{-4}				
66.3	4.46×10^{-4}				
67.3	4.30×10^{-4}				

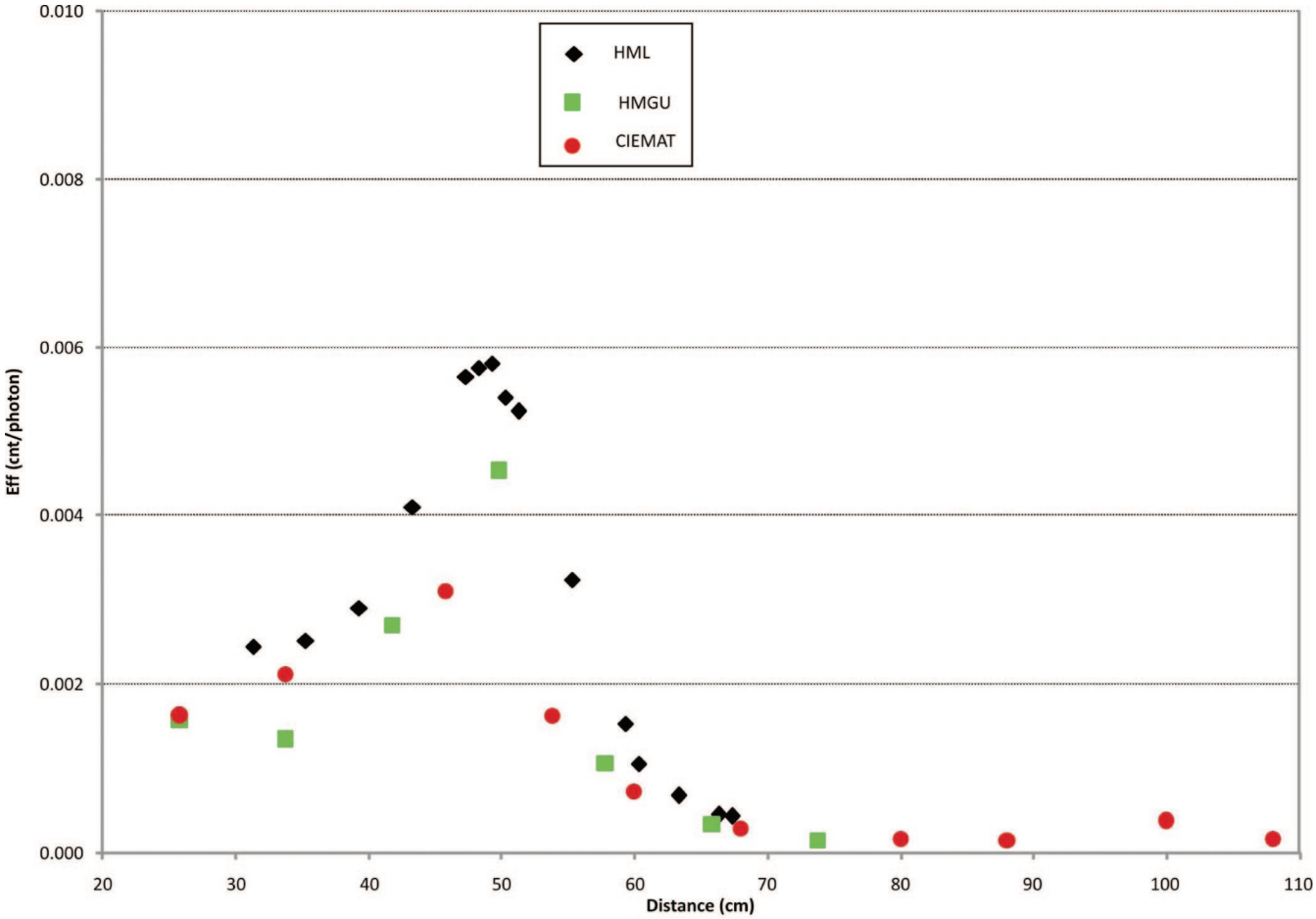

Fig. 8. Counting efficiencies of the USTUR leg phantom as a function of distance from the foot.

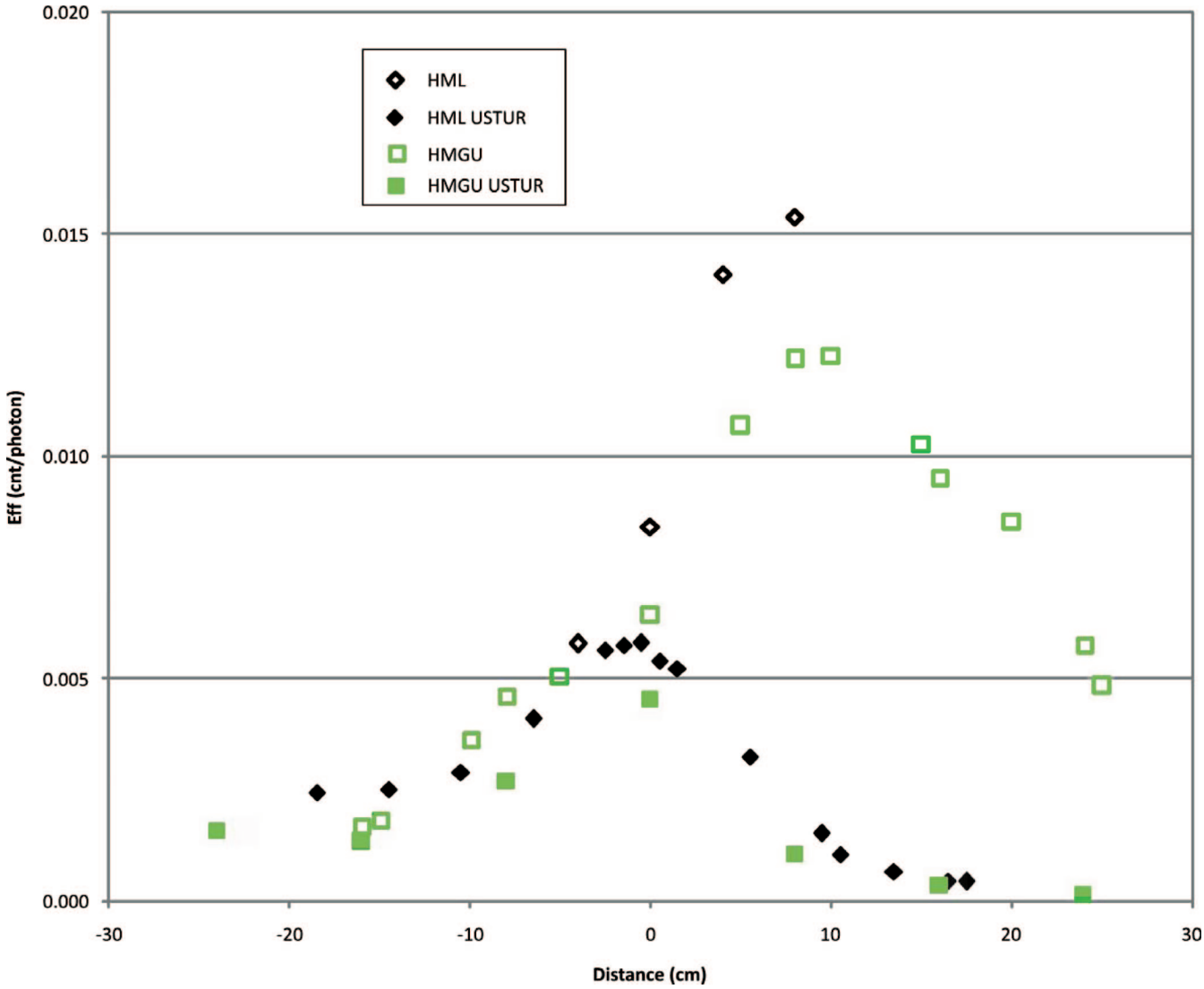

Fig. 9. Efficiency patterns of the two phantoms using the HML and HMGU data. The USTUR phantom is distinguished from the commercial phantom by adding the acronym to the facility name.

resulted in a different approach for optimization counting efficiency compared with the commercial calibration phantom, where the maximum 59.5 keV photon fluence was obtained in the lower segment of the knee.

Table 2 and Fig. 7 show the results of measuring the commercial knee phantom at each of the three facilities (HML, HMGU, and CIEMAT). Table 3 and Fig. 8 show the results of counting the USTUR leg phantom at these facilities. The results are expressed in terms of counts per second per photon per second (or counts per photon). A branching ratio of 0.363 for the 59.5 keV photons was used to make this conversion (Ortec 2010b).

The HML's data show that the counting efficiency of the commercial leg phantom rises as the detector is moved down the leg from 4 cm above the knee to 8 cm below the knee.In contrast, the counting efficiency of the USTUR leg phantom peaks at the kneecap, and at 8 cm below the knee the counting efficiency has dropped by a factor of about 1.8. Both HMGU and CIEMAT's results mirror this finding.

Comparing the results obtained with the commercial and the USTUR phantoms, one sees that the most efficient counting positions for the commercial phantoms are well below the knee. Table 2 shows that HML found it to be 8 cm, HMGU found it to be between 8 and 10 cm, and CIEMAT only provided results for the 4 cm point. In contrast, for the USTUR phantom, Table 3 shows that the most efficient counting position found by HML was at 49.3 cm. HMGU found it to be at 49.8 cm, and CIEMAT found it to be between 45.8 and 53.8 cm. The position of

the patella in the USTUR phantom is at 50 cm from the foot, meaning that the most efficient counting position is approximately 8 cm higher up the leg than the commercial leg phantom. Fig. 9 shows the difference between the two phantoms very clearly using the HML and HGMU data. Here it can be seen that the maximum counting efficiency for each phantom is in very different places along the leg and that the value of that counting efficiency is not consistent between the two phantoms. This difference occurs as one phantom has an activity distribution resulting from ^{241}Am being metabolized into the bone matrix, while the commercial phantom has had the activity added to the bone substitute material.

The differences between the two phantoms may best be shown by the following analysis. If, for example, the HMGU counting system were calibrated using the commercial phantom and (as the most natural choice) the position of the knee cap were chosen as a reference, then a counting efficiency of 7.16×10^{-3} (cnt photon^{-1}) would be obtained (mean of 6.46×10^{-3} and 7.85×10^{-3}; Table 2). In contrast, the USTUR phantom would give only a counting efficiency of 4.52×10^{-3} (cnt photon^{-1}) for the same counting position (Table 3). In other words, if the calibration of ^{241}Am in bone were obtained from the commercial phantom, then one would estimate an activity in the USTUR leg phantom of about 740 Bq instead of the actual 1,190 Bq. This difference of a factor of 0.6 is simply due to the fact that the distribution of ^{241}Am in the two phantoms is different. If the maximum efficiency obtained from the commercial phantom were used instead (1.23×10^{-2}; Table 2), an activity of 434 Bq would result, and the agreement is even worse (factor of 0.35). These differences are likely due to a number of factors: different distribution of ^{241}Am in the bone surface and/or volume and variations between bones or different bone/patella anatomy. Phantoms produced artificially may not be the best calibration choice if a real contamination case is to be measured, as the artificial phantom will inadequately simulate the outcome of a person's metabolic processes.

CONCLUSION

The comparison of a commercially-available leg phantom in which the activity has been artificially distributed with a leg phantom in which the activity has been deposited through normal metabolic processes shows a distinct difference in the activity distribution between the two phantoms. An error in the activity estimate can be quite large if the commercial leg phantom is used to estimate what is contained in the USTUR leg phantom and, consequently, a real person. As the latter phantom was created as a result of a real contamination, it is deemed to be the more representative of what would actually happen if a person were internally contaminated with ^{241}Am. Thus it is concluded that, whenever available, a naturally-contaminated phantom should be used rather than artificially-contaminated ones. It is clear, however, that those naturally-contaminated phantoms are very rare as they require body donations of contaminated individuals. To the best of the authors' knowledge, USTUR is one of the very few places worldwide (if not the only one) where such naturally-contaminated phantoms can be and have already been produced. This demonstrates the unique position USTUR has to support in vivo counting techniques developed for actinide measurements and help internal dosimetrists make the best possible dose estimate, which in turn estimates the best possible health risk that might be associated with incorporated radionuclides.

REFERENCES

Breitenstein BD, Newton CE, Norris HT, Heid KR, Robinson B, Palmer HE, Rieksts GA, Spitz HB, McInroy JF, Boyd HA, Eutsler BC, Romero D, Durbin PW, Schmidt CT. The U.S. Transuranium Registry report on the ^{241}Am count of a whole body. Health Phys 49:559–648; 1985.

Canberra. Systems for in vivo activity measurement [online]. 2010. Available at www.canberra.com/products/536.asp. Accessed 20 December 2010.

Daka JN, Kramer GH. The Canadian National Calibration Reference Centre for Bioassay and In Vivo Monitoring: an update. Health Phys 97:590–594; 2009.

Hickman DP, Cohen N. Reconstruction of a human skull calibration phantom using bone sections from an ^{241}Am exposure case. Health Phys 55:59–65; 1988.

Kramer GH, Limson Zamora M. The Canadian National Calibration Reference Centre for Bioassay and In Vivo Monitoring: a program summary. Health Phys 67:192–196; 1994.

Lopez MA, Navarro JF, Navarro T, Gómez Ros JM, Moraleda M. In-vivo calibration of a LEGe detection system for the assessment of americium in bone in the whole body counter of CIEMAT. In: Proceedings of the IRPA11 Congress, Madrid, Spain, 23–28 May 2004. Fontenay-aux-Roses, France: IRPA; Paper 3a26; 2004.

Lopez MA, Broggio D, Capello K, Cardenas-Mendez E, El-Faramawy N, Franck D, James AC, Kramer GH, Lacerenza G, Lynch TP, Navarro JF, Navarro T, Perez B, Rühm W, Tolmachev SY, Weitzenegger E. EURADOS intercomparison on measurements and Monte Carlo modeling for the assessment of americium in a USTUR leg phantom. Radiat Protect Dosim 144:295–299; 2011.

Lynch TP. Distribution of plutonium and americium in four human skeletons. Seattle: University of Washington; 1988. Thesis.

Moraleda M, Gomez-Ros JM, Lopez MA, Navarro T, Navarro JF. A Monte Carlo-based phantom for in vivo measurements of ^{241}Am in bone. Nucl Instr Meth Phys Res A 538:731–737; 2005.

Navarro JF, Lopez MA, Navarro T, Gómez Ros JM, Moraleda M. Assessment of the internal dose of ^{241}Am in bone by in

vivo measurement of the activity deposited in knee. Radiation Protection Dosimetry 127:531–534; 2007.

Ortec. Whole-body counting [online]. 2010a. Available at www.ortec-online.com/Solutions/whole-body-counters.aspx. Accessed 20 December 2010.

Ortec. Nuclide Navigator v 3.4 [online]. 2010b. Available at www.ortec-online.com. Accessed 20 December 2010.

Spitz H, Jenkins M, Lodwick J, Bornschein R. A new anthropometric phantom for calibrating in vivo measurements of stable lead in the human leg using x-ray fluorescence. Health Phys 78:159–169; 2000.

United States Department of Energy. Phantom library [online]. 2009. Available at www.pnl.gov/phantom/. Accessed 6 October 2009.

United States Transuranium and Uranium Registries. USTUR 0102: University of California—1952-4 Wound, chronic inhalation—$^{241}AmO_2$: narrative. United States Transuranium and Uranium Registries. Washington State University: College of Pharmacy; 2009. Available at www.ustur.wsu.edu/Case_Studies/Narratives/0102_Gunn.php. Accessed 30 August 2010.

United States Transuranium and Uranium Registries. USTUR 0102: University of California—1952-4 Wound, chronic inhalation—$^{241}AmO_2$: radiochemistry. Washington State University: College of Pharmacy; 2010; Available at www.ustur.wsu.edu/Case_Studies/Radiochemistry/xls/0102_RadChem_Rev.1.xls. Accessed 30 August 2010.

Wahl W, Roth P, Haninger T, Kucheida D. Reconstruction of individual cumulative radon exposure by low level in vivo measurements and biokinetic modeling. J Radioanalytical Nucl Chem 252:255–259; 2002.

■ ■